Trophic pathways of phytoplankton size classes through the zooplankton food web over the spring transition period in the north-west Mediterranean Sea

Brian Hunt, Francois Carlotti, Katty Donoso, Marc Pagano, Fabrizio d'Ortenzio, Vincent Taillandier, Pascal Conan

Key Points:
- Picoplankton was estimated to contribute >60% to total zooplankton biomass in oligotrophic regions of the north-west Mediterranean
- Picoplankton, nanoplankton, and microplankton were estimated to contribute 42, 42, and 20%, respectively, to total zooplankton biomass in the eutrophic deep convection zone
- The contribution of diatoms to zooplankton diets may be overestimated in eutrophic food webs

Supporting Information:
- Supporting Information S1

Correspondence to:
B. P. V. Hunt,
b.hunt@oceans.ubc.ca

Trophic pathways of phytoplankton size classes through the zooplankton food web over the spring transition period in the north-west Mediterranean Sea

Brian P. V. Hunt[1,2,3] [iD], **François Carlotti[3]**, **Katty Donoso[3]** [iD], **Marc Pagano[3]**, **Fabrizio D'Ortenzio[4]** [iD], **Vincent Taillandier[4]** [iD], **and Pascal Conan[5]** [iD]

[1]University of British Columbia, Institute for the Oceans and Fisheries, Vancouver, British Columbia, Canada, [2]Hakai Institute, Heriot Bay, British Columbia, Canada, [3]Aix-Marseille Univ, Univ Toulon, CNRS, IRD, MIO UM 110, Mediterranean Institute of Oceanography, Marseille, France, [4]Sorbonne Universités, UPMC Univ Paris 06, CNRS, Laboratoire d'Océanographie de Villefranche CNRS-UPMC, UMR 7093, France, [5]Sorbonne Universités, UPMC Univ Paris 06, CNRS, UMR7621, Laboratoire d'Océanographie Microbienne, Observatoire Océanologique, Banyuls/mer, France

Abstract Knowledge of the relative contributions of phytoplankton size classes to zooplankton biomass is necessary to understand food-web functioning and response to climate change. During the Deep Water formation Experiment (DEWEX), conducted in the north-west Mediterranean Sea in winter (February) and spring (April) of 2013, we investigated phytoplankton-zooplankton trophic links in contrasting oligotrophic and eutrophic conditions. Size fractionated particulate matter (pico-POM, nano-POM, and micro-POM) and zooplankton (64 to >4000 μm) composition and carbon and nitrogen stable isotope ratios were measured inside and outside the nutrient-rich deep convection zone in the central Liguro-Provencal basin. In winter, phytoplankton biomass was low (0.28 mg m^{-3}) and evenly spread among picophytoplankton, nanophytoplankton, and microphytoplankton. Using an isotope mixing model, we estimated average contributions to zooplankton biomass by pico-POM, nano-POM, and micro-POM of 28, 59, and 15%, respectively. In spring, the nutrient poor region outside the convection zone had low phytoplankton biomass (0.58 mg m^{-3}) and was dominated by pico/nanophytoplankton. Estimated average contributions to zooplankton biomass by pico-POM, nano-POM, and micro-POM were 64, 28 and 10%, respectively, although the model did not differentiate well between pico-POM and nano-POM in this region. In the deep convection zone, spring phytoplankton biomass was high (1.34 mg m^{-3}) and dominated by micro/nano phytoplankton. Estimated average contributions to zooplankton biomass by pico-POM, nano-POM, and micro-POM were 42, 42, and 20%, respectively, indicating that a large part of the microphytoplankton biomass may have remained ungrazed.

Plain Language Summary The grazing of zooplankton on algal phytoplankton is a critical step in the transfer of energy through all ocean food webs. Although microscopic, phytoplankton span an enormous size range. The smallest picophytoplankton are generally thought to be too small to be directly grazed by zooplankton, resulting in less efficient energy transfer through the food web. This has implications for our future oceans where warming and lower nutrient supply are predicted to favor picophytoplankton over the larger nanosize and microsize classes. We tested the importance of phytoplankton size classes in the transfer of energy to zooplankton in the north-west Mediterranean Sea, where conditions naturally result in contrasting regions of small and large phytoplankton dominance. Contrary to expectation, biochemical tracers showed that microphytoplankton never contributed more than 20% to zooplankton biomass, even in regions where microphytoplankton were plentiful. On the other hand, picophytoplankton contributed 25–65% to zooplankton biomass. This finding indicates that there are well-established food-web pathways from picophytoplankton to zooplankton, and that these pathways play an important role even in ocean regions where microphytoplankton dominate. Accordingly, a decline in phytoplankton size classes may have a greater effect on carbon sequestration than on food-web productivity.

1. Introduction

Organism size is a key factor in food-web dynamics. Consumers tend to ingest organisms 1 order of magnitude smaller than themselves [*Cohen et al.*, 1993; *Sheldon et al.*, 1972]. Meta-analysis of feeding linkages across a range of terrestrial and marine habitats shows that in 90% of cases predators are larger than prey [*Barnes et al.*, 2010; *Cohen et al.*, 1993]. The size structure of phytoplankton communities is therefore expected to be a key property of pelagic food webs. Phytoplankton length and volumetric size span a range of 4 and 9 orders of magnitude, respectively [*Finkel et al.*, 2010]. They can be broadly ordered into three size classes: pico (<2 μm), nano (2–20 μm), and micro (20–200 μm) [*Azam et al.*, 1983]. The picophytoplankton is considered to be too small to be effectively grazed by most metazoans [*Fortier et al.*, 1994], including copepods, the oceans dominant zooplankton grazers and the major pathway for primary production to higher trophic levels [*Legendre and Rassoulzadegen*, 1995; *Ryther*, 1969]. In picophytoplankton-dominated systems, it has been estimated that ∼50% of the autotrophic energy that enters the "copepod pathway" does so via feeding on intermediary microzooplankton grazers, including heterotrophic flagellates and ciliates [*Calbet and Landry*, 1999; *Calbet and Saiz*, 2005; *Sommer et al.*, 2002]. Conversely, the nanophytoplankton and microphytoplankton size classes are accessible to zooplankton grazers and in systems where these phytoplankton groups dominate ∼75% of the energy entering the "copepod pathway" is estimated to occur via direct phytoplankton herbivory [*Calbet and Saiz*, 2005].

The size structure of phytoplankton communities therefore has implications for food chain length and, following the rules of ecological efficiency, the energy transfer efficiency to zooplankton [*Sommer et al.*, 2002]. Specifically, a gradient of low to high transfer efficiency is expected with an increasing contribution of larger phytoplankton size classes. Globally, picophytoplankton dominate in oligotrophic regions and nutrient-rich regions that are light and/or iron limited, while microphytoplankton dominate in naturally eutrophic (nutrient-rich) regions [*Kiorboe*, 1993; *Uitz et al.*, 2010]. Consequently, phytoplankton size composition has significant implications for regional differences in food-web structure. It is also an important consideration in the context of long-term change as enhanced stratification and decreased nutrient supply to the photic zone, favoring picophytoplankton, is predicted with ongoing ocean warming [*Ganachaud et al.*, 2013; *Moran et al.*, 2010; *Polovina et al.*, 2011].

Our current understanding of the pathways and contributions of picophytoplankton, nanophytoplankton, and microphytoplankton size classes, and microzooplankton, to the zooplankton food web has largely been informed by experimental studies, including small volume incubations and mesocosms [*Atkinson*, 1996; *Calbet and Landry*, 2004; *Calbet and Saiz*, 2005; *Fileman et al.*, 2014; *Lewandowska and Sommer*, 2010]. More recently, molecular analyses have opened up the possibility of highly resolved studies of zooplankton diet composition [*Craig et al.*, 2014; *Durbin and Casas*, 2014]. In situ observations have largely been through predator-prey correlation [*Boyce et al.*, 2015], however, biochemical approaches provide a means to measure time-integrated consumption of phytoplankton groups by zooplankton. Fatty acid analyses have been used to determine grazing by zooplankton on phytoplankton groups [*El-Sabaawi et al.*, 2009; *Schukat et al.*, 2014] and size fractions [*Escribano and Pérez*, 2010; *Rossi et al.*, 2006]. Analysis of naturally occurring stable isotope ratios has been extensively applied to examine food-web linkages among consumers [*Hobson and Welch*, 1992; *Wada et al.*, 1991], however, due to sample size requirements, few studies have attempted to use this approach to resolve linkages between zooplankton and lower trophic levels. The studies that have measured the isotope ratios of pico-sized, nano-sized, and micro-sized particulates have demonstrated clear differences between size classes and the suitability of this approach to interpretation of plankton food-web dynamics [*Im and Suh*, 2016; *Karsh et al.*, 2003; *Rau et al.*, 1990; *Rautio and Vincent*, 2007; *Tiselius and Fransson*, 2016; *Waite et al.*, 2007]. A caveat with the particulate size fractionation approach is that it does not separate the autotrophic and heterotrophic components of the measured size fractions. Recent research provides evidence that there may be little isotopic fractionation between phytoplankton and microzooplankton [*Gutiérrez-Rodríguez et al.*, 2014], in which case the isotope values of picoplankton, nanoplankton, and microplankton size fractions would be expected to largely reflect that of the autotrophic components. An advantage of the stable isotope approach is that, since the signatures of the zooplankton reflect assimilated prey biomass, with knowledge of consumer and particulate matter size fraction isotope values it is possible to estimate the relative contribution of these size fractions to zooplankton biomass [*Phillips et al.*, 2014].

The Mediterranean Sea is considered to be broadly oligotrophic, with a west to east gradient of decreasing phytoplankton biomass reflecting the gradient of available nutrients [*D'Ortenzio and Ribera d'Alcalà*, 2009].

Nanophytoplankton and picophytoplankton dominate the phytoplankton community with the exception of regions of nutrient enhancement where diatoms can make a large contribution to phytoplankton biomass [*Marty et al.*, 2002; *Siokou-Frangou et al.*, 2010]. One such region is the Liguro-Provencal Basin in the north-west Mediterranean [*D'Ortenzio and Ribera d'Alcalà*, 2009]. Here an annual spring phytoplankton bloom is observed, supported by deep winter convection that brings nutrients to the surface and stimulated by spring warming and stratification of the surface ocean [*Estrada et al.*, 2014]. In 2013, the Deep Water formation Experiment (DEWEX) set out to improve understanding of the north-west Mediterranean Sea ecosystem and the relative functioning of the regions in and outside the deep convection zone. Two extensive biooceanographic surveys were completed in winter and spring. We used this research platform to investigate the seasonal development of the zooplankton food-web dynamics in contrasting regions of high and low productivity, with high and low microphytoplankton biomass, respectively. Using stable isotope analysis and a mixing model approach, we specifically aimed to determine the relative contributions of picoplankton, nanoplankton, and microplankton to zooplankton biomass in these contrasting trophic regimes.

2. Materials and Methods

2.1. Field Program
The two DEWEX cruises were conducted onboard the R/V Le Suroît in 2013, from 3 to 21 February during the winter deep convection period, and from 5 to 24 April during the spring bloom. A star-shaped survey grid sampling the cyclonic circulation of the basin was employed, comprising 76 stations on Leg 1 and 100 stations on Leg 2 (Figure 1).

2.1.1. Environmental Data
A CTD (SeaBird Electronics' 911+ technology) mounted on a 12 bottle rosette (12L Niskin bottles) was deployed at each station. Fluorescence profiles were measured using a Chelsea fluorometer. Discrete depth water samples were collected though the water column (5 depths < 100 m) for analysis of nutrients (nitrate + nitrite, silicate, and phosphate), phytoplankton pigment concentrations, and for microscopic analysis of nanoflagellate, dinoflagellate, and microzooplankton concentrations. Phytoplankton pigment analysis was through high-performance liquid chromatography (HPLC), the procedure for which is described in detail in *Mayot et al.* [2017]. The chlorophyll *a* biomass (μg L^{-1}) associated with the microphytoplankton, nanophytoplankton, and picophytoplankton size classes was estimated through multiple regression using seven diagnostic pigments as predictors, following *Uitz et al.* [2006].

2.1.2. Zooplankton Sampling
Zooplankton sampling was conducted at night using a 70 cm Bongo net fitted with 64 and 120 μm mesh (sample locations are illustrated on the map in Figure 1). At each zooplankton station, two vertical net hauls were completed between 250 m and the surface, with a hauling speed of 1 m s^{-1}. No flowmeter was used and sampled volume was calculated as a product of the net diameter and net depth (i.e., 0.38 m^2 $\times$ 250 m = 95 m^3), assuming that the net sampled with 100% efficiency. For this study, only the 64 μm mesh samples were used. The first net haul was preserved in a 10% formalin-seawater solution for taxonomic analysis. The second net haul was size fractionated by sieving through a sieve column comprising 4000, 2000, 1000, 500, 250, 125, and 64 μm mesh sieves. With the exception of the 4000 μm sieve, the contents of each sieve were washed into separate beakers using a spray bottle filled with 0.7 μm filtered seawater. Subsequently, the contents of each beaker were filtered onto precombusted 47 mm GF/F filters and frozen at -20°C for stable isotope analysis. Organisms in the 4000 μm sieve fraction were, separated into orders, measured to the nearest mm, and stored in Eppendorf tubes at -20°C for stable isotope analysis.

2.1.3. Particulate Organic Matter (POM) Sampling
Size fractionated POM samples were collected at select stations for stable isotope analysis. Four stations were sampled on Leg 1, and 11 stations on Leg 2 (5 in the convection zone and 6 outside the convection zone). At each POM station, 20 L of water was collected from the chlorophyll *a* maximum identified from the fluorescence signal of the CTD downcast. When no chlorophyll *a* maximum was discernable then the water for POM was collected from 20 m depth. The water was prescreened through a 64 μm sieve and then serial filtered at a pressure of $\sim$0.2 bar through a 47 mm 20 μm nitex filter, 142 mm 2 μm polycarbonate filter, and a 47 mm precombusted GF/F filter ($\sim$0.7 μm). The contents of the 20 and 2 μm filters were gently washed into separate beakers using a spray bottle filled with 0.7 μm filtered seawater. Subsequently, the contents of each beaker were filtered onto separate precombusted 47 mm GF/F filters. Precombustion of GF/F filters was at 450°C for 4 h. Samples were stored frozen at -20°C for stable isotope analysis.
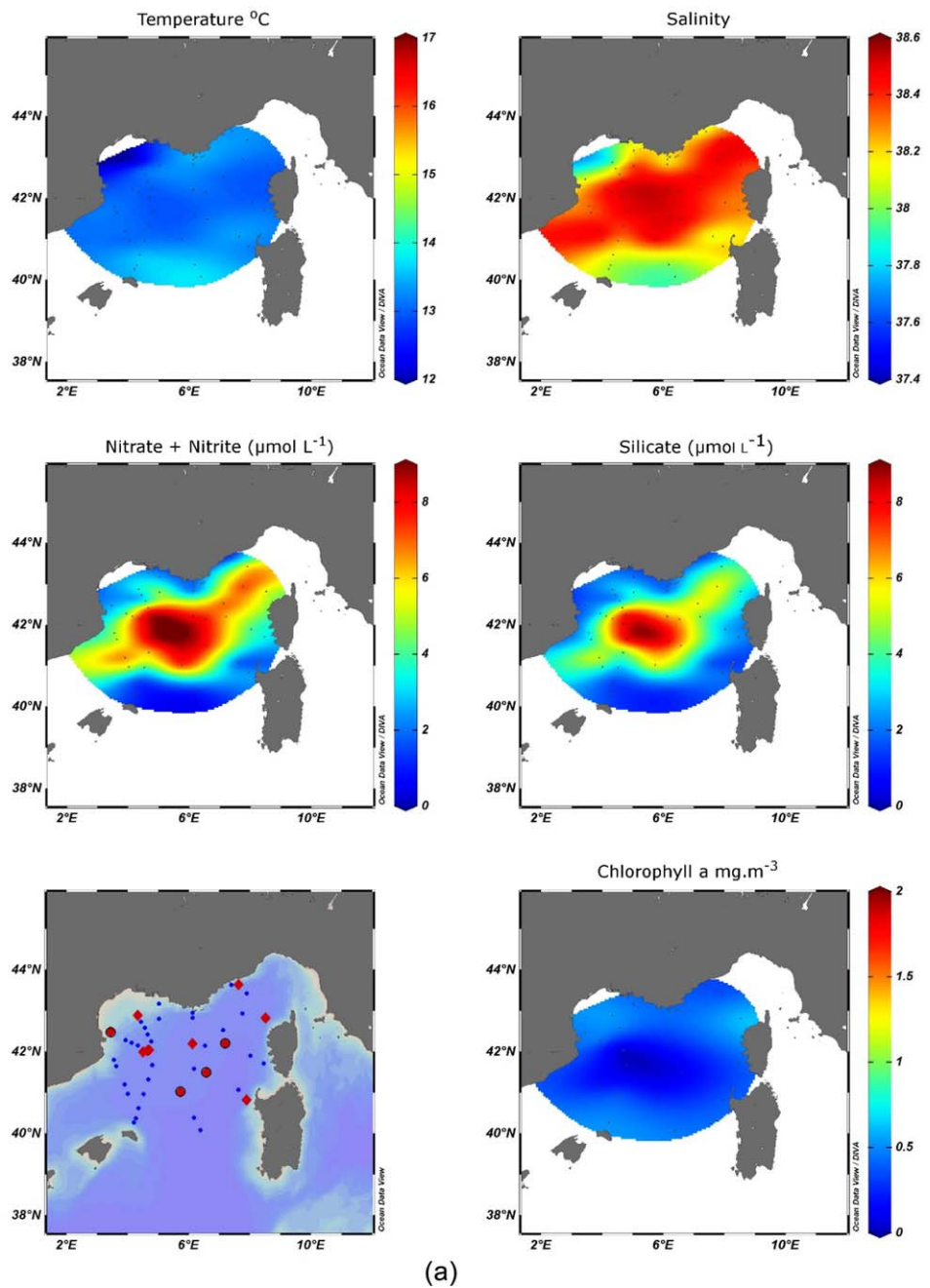
Figure 1. (continued)

2.2. Laboratory Processing

2.2.1. Zooplankton Taxonomic Identification

Formalin-preserved samples were used for taxonomic analysis of the zooplankton community. Analysis was performed under a stereo microscope, from a 1/8 to 1/16 fraction of each sample. Specimens were identified to the level of order and enumerated. An average of 960 individuals was counted per sample and we estimated an enumeration error of 6.4% [*Gifford and Caron*, 2000]. The category copepod nauplii comprised a mix of calanoid, cyclopoid, and poecilostomatoid copepods. Counts were converted to densities expressed as individuals m^{-3}.

2.2.2. Stable Isotope Analysis

POM and zooplankton samples for stable isotope analysis were first dried at 50°C for 48 h. Zooplankton samples were weighed to the nearest 0.01 mg using a microbalance and values converted to mg Dry
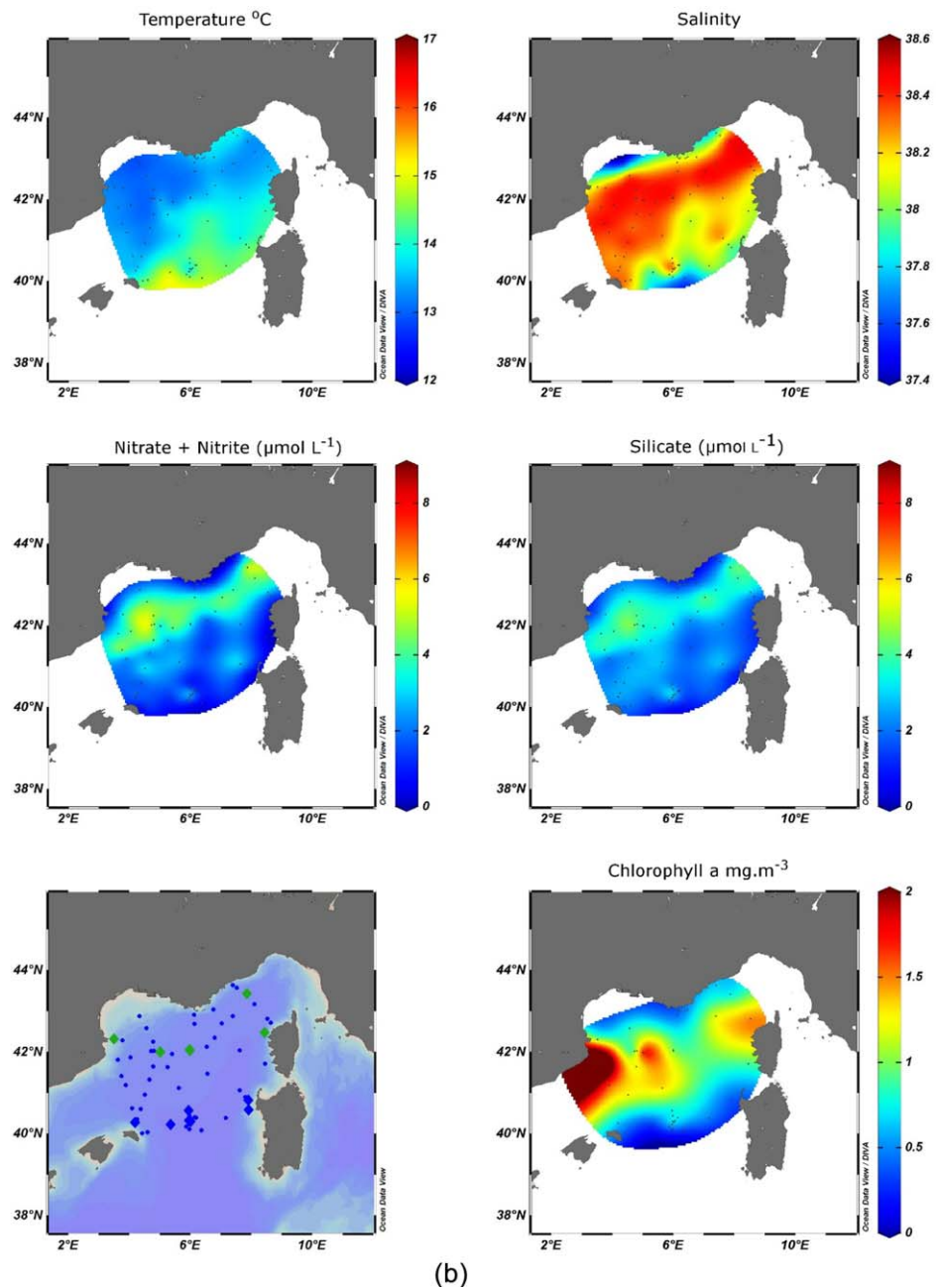
Figure 1. Distribution of environmental variables during (a) Leg 1 and (b) Leg 2 of the DEWEX program. The location of oceanographic stations is indicated by small blue dots. Winter zooplankton stations are indicated by red dots (a), SpringHB (convection zone) by large blue dots and SpringLB (outside convection zone) by green dots.

Weight (DW) m^{-3}. Zooplankton were subsequently removed from the GF/F filter, homogenized using a mortar and pestle, and ∼1 mg subsamples packaged into tin cups. The surface of POM filters was peeled and packaged directly into tin cups. Stable isotope analysis of the POM and zooplankton samples was performed at the IsoEnvironmental Laboratory (http://www.isoenviron.co.za/), Rhodes University, South Africa, with a Europa Scientific 20–20 isotope ratio mass spectrometer (IRMS) linked to a preparation unit (ANCA SL). Casein and a mixture of beet sugar and ammonium sulphate were used as internal standards and were calibrated against the International Atomic Energy Agency (IAEA) standards CH-6 and N-1) and the IRMS certified reference material EMA-P2 (see Certificate BN/132357). $\delta^{13}C$ and $\delta^{15}N$ values were determined in parts per thousand (‰) relative to external standards of Vienna Pee Dee Belemnite and atmospheric N.

Repeated measurements (after every third sample) of an internal standard indicated measurement precision of $\pm 0.09\permil$ and $\pm 0.19\permil$ for $\delta^{13}C$ and $\delta^{15}N$ values, respectively.

2.3. Statistical Analysis

Surface plots of physical, chemical, and biological data averaged through the upper 100 m of the water column were generated for each DEWEX leg (Figure 1). Variance in parameters among zooplankton stations in winter, the spring deep convection zone (northern stations with chl a biomass > 0.8 mg m^{-3}—hereafter Spring High Biomass, i.e., SpringHB), and spring stations outside the convection zone (southern stations with chl a biomass < 0.8 mg m^{-3}—hereafter Spring Low Biomass, i.e., SpringLB) was tested using ANOVA. Nanoflagellate, dinoflagellate, and microzooplankton densities and zooplankton biomass were log transformed prior to analysis. Where significant differences were detected a post hoc Tukey HSD test was run to test for differences among regions.

A sample by taxon matrix was created using taxon specific densities. Densities were $\log_{10}(x + 1)$ transformed and the percentage similarity between stations from all surveys was calculated using the Bray-Curtis similarity index [*Field et al.*, 1982]. The similarity matrix was then ordinated using nonmetric multidimensional scaling (NMDS), summarizing between sample variation in community composition into two dimensions. These multivariate analyses were performed using PRIMER 6 [*Clarke and Warwick*, 2001]. The NMDS ordination had a stress value of 0.16.

The percent contribution of POM to zooplankton size classes was estimated using a Bayesian mixing model framework [*Parnell et al.*, 2013], based on tissue $\delta^{15}N$ and $\delta^{13}C$ values. Models were implemented using the R package simmr [*R Core Team*, 2016]. This modeling approach incorporates source variability and generates probability distributions of likely diet contributions. Trophic discrimination factors (TDFs) are an important source of variability in mixing model estimates. There is no well-established set of TDFs for plankton and as such we computed mixing model estimates using the mean TDF values from a global meta-analysis: 2.75 (± 0.1) for $\delta^{15}N$ and 0.75 (± 0.11) for $\delta^{13}C$ [*Caut et al.*, 2009].

3. Results

3.1. Environmental Conditions

The impact of winter convection in the central Liguro-Provencal Basin was clearly evident in the distribution of high salinity and high nutrient concentrations in the upper 100 m of the water column, indicative of deep water (Figure 1a and Table 1). Winter temperature was comparatively homogenous across the survey area reflecting the dual effects of surface cooling and convection, and phytoplankton biomass was uniformly low. Conditions changed quite markedly in the spring. The convection zone retained high salinity and relatively high nutrients, although the latter were depleted relative to winter levels due to an extensive phytoplankton bloom, evident in the high phytoplankton (chl a) biomass in that region (Figure 1b). Phytoplankton biomass was significantly higher in SpringHB stations, which corresponded with the convection

Table 1. Average $\pm$ Standard Deviations of Environmental Variables in Winter, SpringHB, and SpringLB[a]

Variables	Winter (n = 10)	SpringHB (n = 6)	SpringLB (n = 7)	p
Temperature (°C)	13.07 $\pm$ 0.18 a	13.39 $\pm$ 0.26 a	14.19 $\pm$ 0.48 b	<0.01
Salinity	38.39 $\pm$ 0.16 a	38.39 $\pm$ 0.12 a	38.17 $\pm$ 0.18 b	<0.01
Silicate (μmol L^{-1})	4.73 $\pm$ 2.38 b	3.33 $\pm$ 0.94 ab	2.34 $\pm$ 0.75 a	<0.05
Phosphate (μmol L^{-1})	0.25 $\pm$ 0.14 b	0.16 $\pm$ 0.06 ab	0.08 $\pm$ 0.04 a	<0.01
NO$_3$ + NO$_2$ (μmol L^{-1})	5.87 $\pm$ 2.69 b	3.48 $\pm$ 1.34 a	1.73 $\pm$ 0.96 a	<0.01
Total chlorophyll a (mg m^{-3})	0.28 $\pm$ 0.19 a	1.34 $\pm$ 0.75 b	0.58 $\pm$ 0.20 a	<0.01
Microphytoplankton (mg m^{-3})	0.09 $\pm$ 0.07 a	0.58 $\pm$ 0.39 b	0.15 $\pm$ 0.08 a	<0.01
Nanophytoplankton (mg m^{-3})	0.11 $\pm$ 0.07 a	0.58 $\pm$ 0.35 b	0.33 $\pm$ 0.12 ab	<0.01
Picophytoplankton (mg m^{-3})	0.07 $\pm$ 0.06 a	0.17 $\pm$ 0.11 a	0.10 $\pm$ 0.01 a	ns
Nanoflagellates (cells L^{-1})	$4.36 \times 10^5 \pm 6.65 \times 10^5$ a	$1.95 \times 10^6 \pm 1.84 \times 10^6$ a	$4.09 \times 10^6 \pm 7.33 \times 10^6$ a	ns
Dinoflagellates (cells L^{-1})	1622.00 $\pm$ 1384.83 a	1666.67 $\pm$ 1860.95 a	13051.33 $\pm$ 26234.01 a	ns
Microzooplankton (cells L^{-1})	656.00 $\pm$ 694.01 a	1240.00 $\pm$ 1363.23 a	531.43 $\pm$ 672.96 a	ns
Zooplankton (dry wt m^{-3})	11.62 $\pm$ 7.54 a	59.65 $\pm$ 46.93 b	28.24 $\pm$ 15.19 b	<0.05
Zooplankton abundance (in d m^{-3})	7827.47 $\pm$ 9665.37 a	16113.63 $\pm$ 10931.22 a	13812.81 $\pm$ 12410.37 a	ns

[a]Differences between regions were tested using ANOVA and Tukey post hoc test. Significant differences between regions are indicated by different letters. Two winter and one SpringHB had no ancillary environmental data and these were excluded from the analysis.
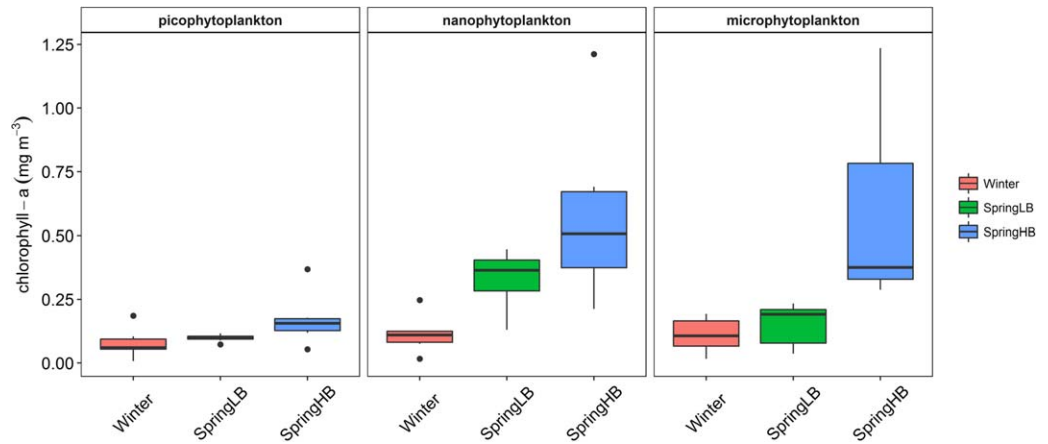
Figure 2. Box plots of size fractionated phytoplankton biomass in winter, SpringLB, and SpringHB. Horizontal bars indicate median proportional values, and the upper and lower edges of the box denote the approximate first and third quartiles, respectively. The vertical error bars extend to the lowest and highest data value inside a range of 1.5 times the interquartile range, respectively. Points indicate extreme values.

zone, than in winter and the SpringLB stations, outside the convection zone (Table 1). Phytoplankton biomass did not differ significantly between winter and SpringLB stations. Microphytoplankton and nanophytoplankton were the major contributors to the high phytoplankton biomass in SpringHB and nanophytoplankton biomass was elevated in SpringLB (Table 1 and Figure 2). Although densities of nanoflagellates, dinoflagellates, and microzooplankton did not differ significantly between regions, nanoflagellates densities were an order of magnitude higher in spring, dinoflagellates occurred at high densities in SpringLB, and microzooplankton densities were highest in SpringHB (Table 1).

3.2. Zooplankton Composition

The NMDS ordination identified distinct zooplankton community composition in Winter, SpringHB, and SpringLB (Figure 3). Similarities within these three station groupings were high (>77%) (supporting
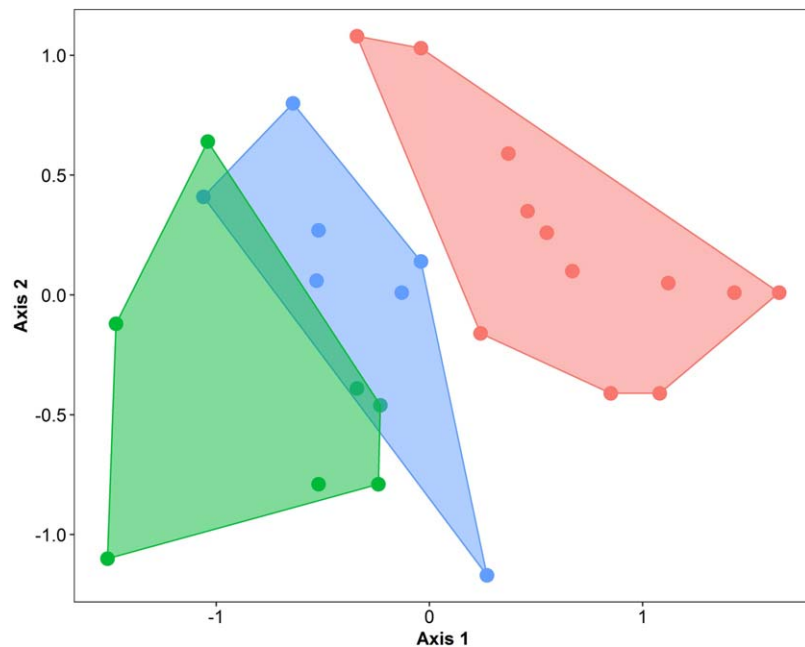

Figure 3. Ordination of zooplankton community composition based on abundance of zooplankton taxa in size classes. Ordination was by NMDS using log transformed abundance data and the Bray-Curtis similarity metric. Station groupings are color coded by region: winter (red), SpringLB (green), and SpringHB (blue).

information Tables S1.1–S1.3). The winter stations had >24% dissimilarity to the two spring surveys, while dissimilarity between the two spring station groupings was ~22% and there was slight overlap at the edges of their respective ordination space. In all cases, differences between station groupings were largely attributed to variation in the abundance of key groups (supporting information Table S1.4).

Overall calanoid copepods were the most abundant group in all regions, followed by cyclopoid and poecilostomatoid copepods. The contribution of taxonomic groups varied between size classes. The 64 μm size class was dominated by copepod nauplii (Figure 4). The 125 μm size class had a large proportion of copepod nauplii, particularly in SpringHB, and cyclopoid, poecilostomatoid, and calanoid copepods were also important. The 250–1000 μm size classes were composed primarily of calanoid copepods. Euphausiids made a relatively important contribution to the 1000 μm size class in SpringLB. During winter, the "other" category, comprising primarily hydromedusae, siphonophores, and chaetognaths, made a large contribution to the 2000 μm size fraction, with a low contribution from calanoid and euphausiids. The "other" group also made a large contribution to the 4000 μm size fraction during winter along with euphausiids. In SpringHB stations, the 2000 μm size fraction composition was similar to that in winter, while the 4000 μm fraction was dominated by tunicates, followed by "other" and euphausiids. Tunicates were the most abundant group in the 2000 and 4000 μm fractions in SpringLB stations.
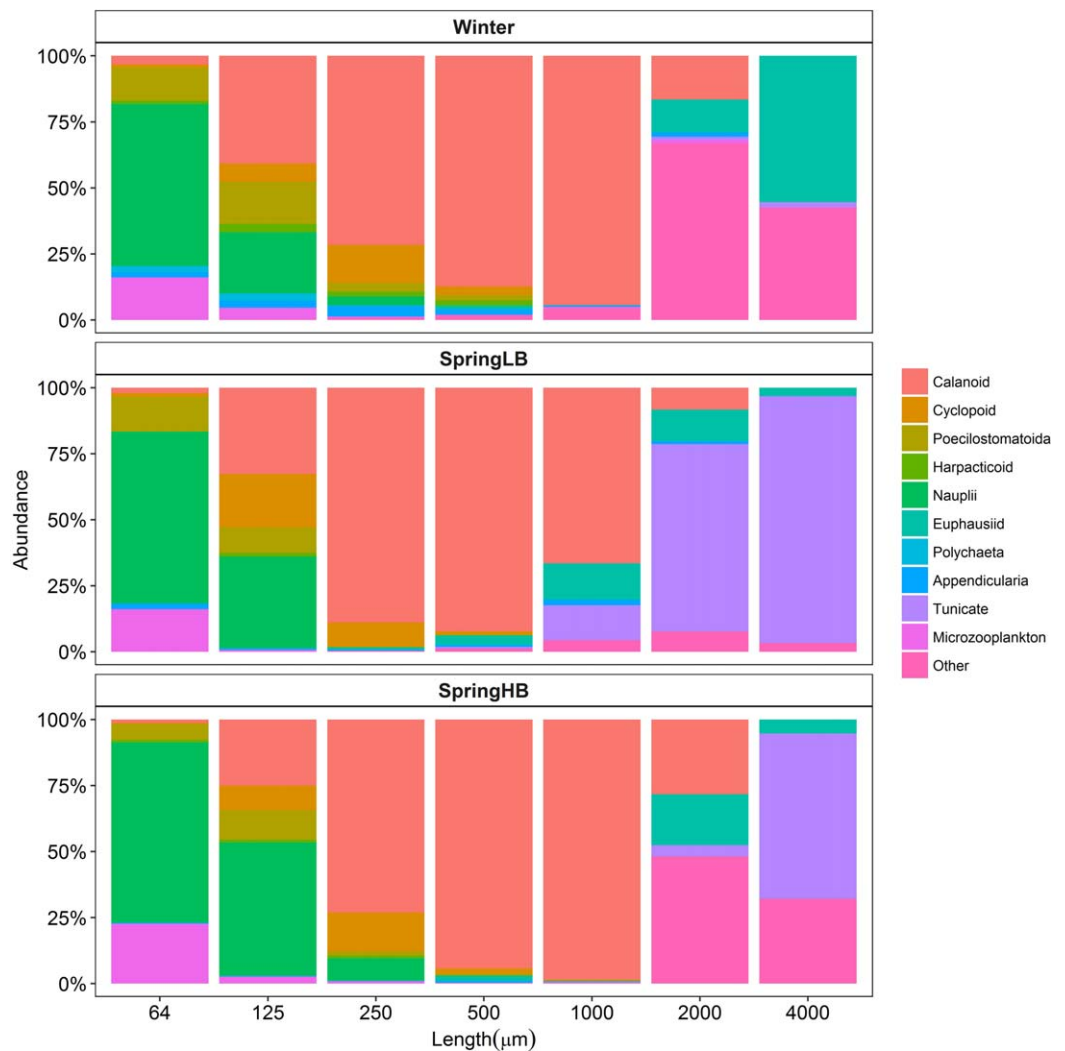

Figure 4. Proportional contribution (abundance) of zooplankton groups to size fractions in winter, SpringLB, and SpringHB. The "microzooplankton" category comprises dinoflagellates, tintinnids, foraminifera, and radiolarians.
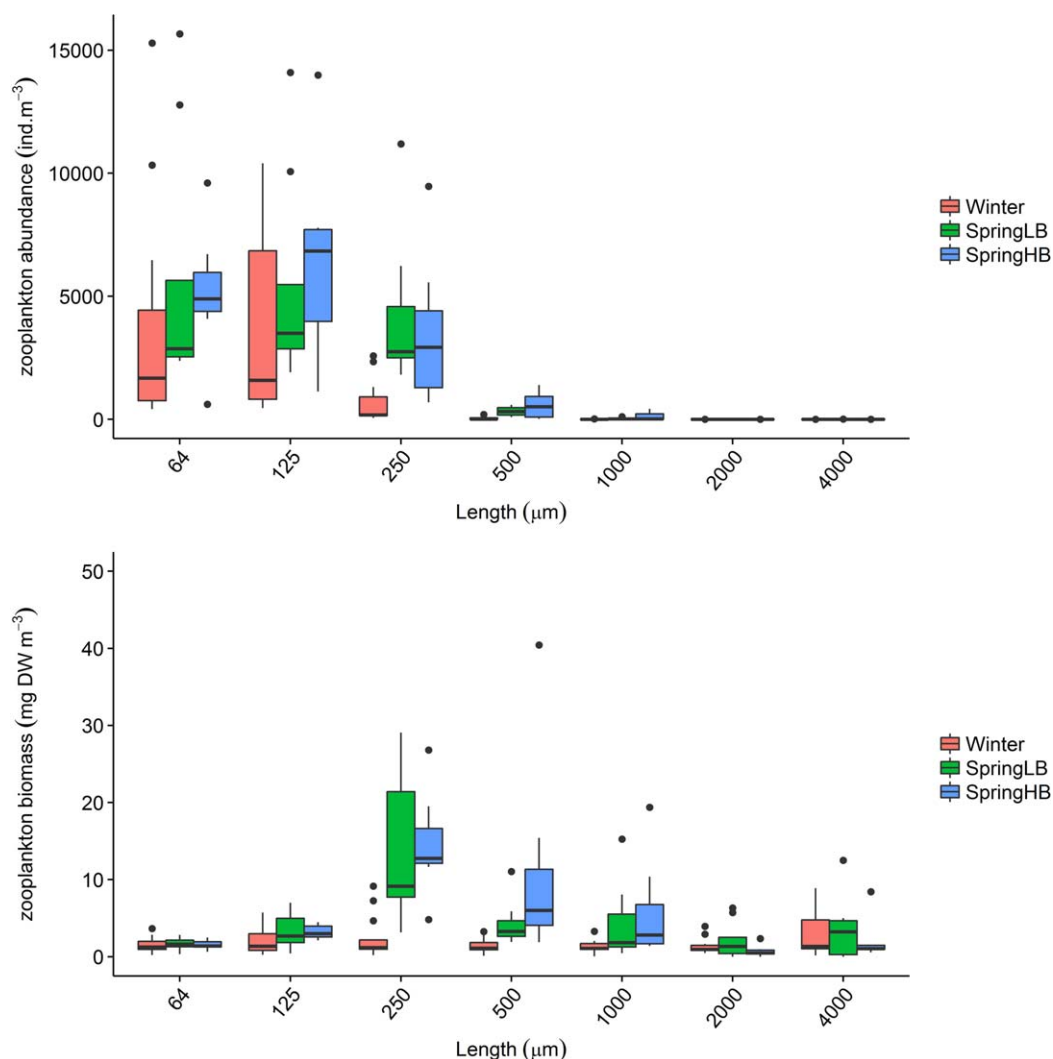
Figure 5. Zooplankton abundance (individuals m^{-3}) and biomass (mg DW m^{-3}) across size classes in winter, SpringLB, and SpringHB. Horizontal bars indicate median proportional values, and the upper and lower edges of the box denote the approximate first and third quartiles, respectively. The vertical error bars extend to the lowest and highest data value inside a range of 1.5 times the interquartile range, respectively. Points indicate extreme values.

Average total station zooplankton abundance did not differ significantly between regions (Table 1). The abundance distribution of zooplankton across size classes was dominated by the 64 and 125 μm size classes in the winter (Figure 5). In the spring, the abundance of the 250 μm increased in both SpringHB and SpringLB. Abundance was comparatively low in size classes >250 μm during both winter and spring. Average total zooplankton biomass was significantly higher in SpringHB and SpringLB than in winter (Table 1). Zooplankton biomass was evenly distributed across size classes in the winter while in the spring biomass peaked in the 250 μm size class and was elevated in the 500 and 1000 μm size classes (Figure 5).

3.3. Stable Isotope Composition of POM and Zooplankton

δ^{15}N differed significantly among POM size fractions (ANOVA; $p < 0.001$). A post hoc Tukey HSD test found that the only pairwise comparison with no significant difference was between the picosize and nanosize fractions ($p = 0.08$). The δ^{15}N values of POM samples were lowest for the picosize fraction (ave. = 0.78‰) and increased with size (Figure 6). In all regions, the range of POM values exceeded that of the zooplankton, and the average value of the 20 μm fraction (5.82‰) was higher than that of the highest average size fraction value in the zooplankton (3.96‰ for euphausiids in SpringLB). Average
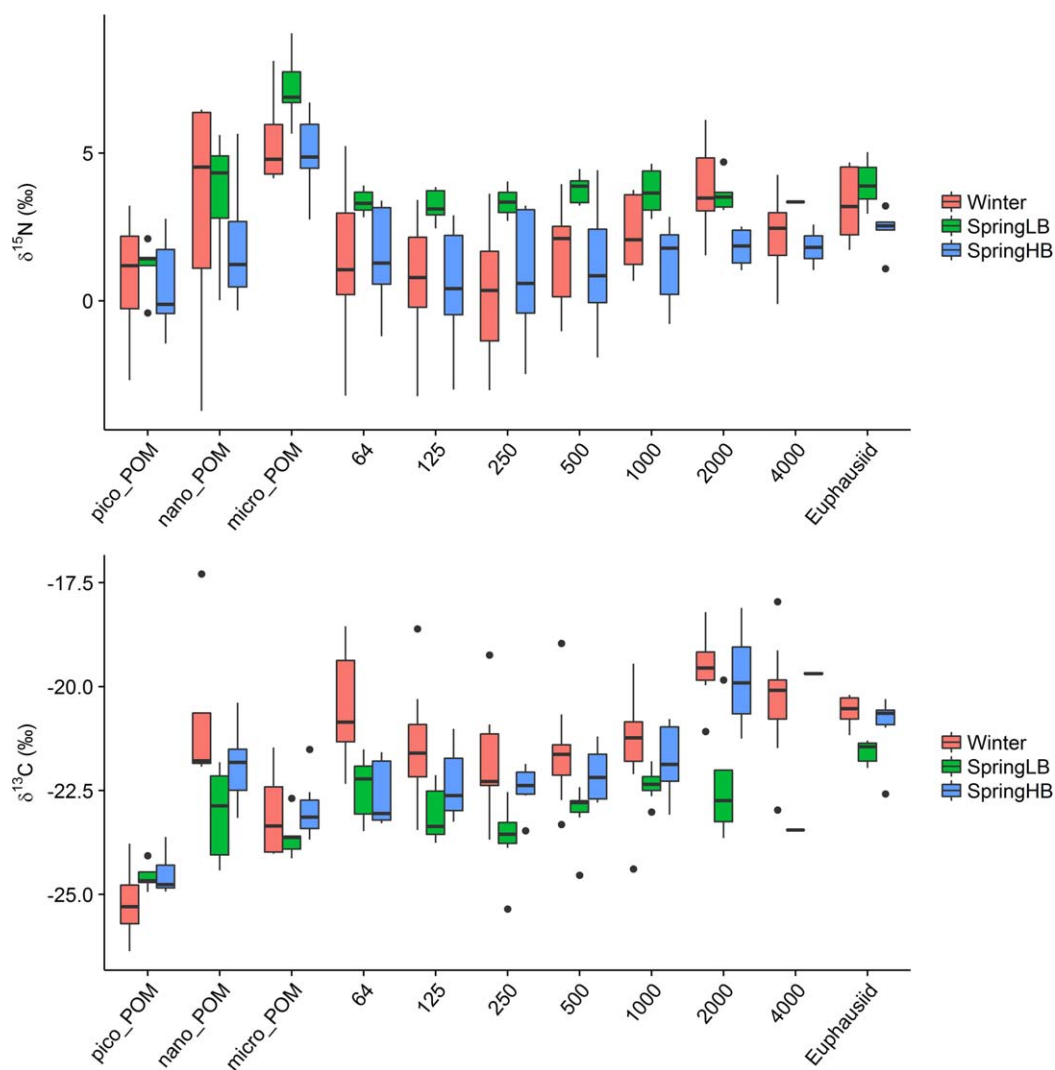
Figure 6. Box plots of δ^{15}N and δ^{13}C for pico, nano, and micro-particulate organic matter (POM), zooplankton size fractions (μm), and euphausiids in winter, SpringLB, and SpringHB. Horizontal bars indicate median proportional values, and the upper and lower edges of the box denote the approximate first and third quartiles, respectively. The vertical error bars extend to the lowest and highest data value inside a range of 1.5 times the interquartile range, respectively. Points indicate extreme values.

zooplankton δ^{15}N values increased weakly with size in winter and SpringHB and varied little across size classes in SpringLB. Average zooplankton δ^{15}N values were 1.71‰ for winter, 1.35‰ for SpringHB, and 3.50‰ for SpringLB.

δ^{13}C differed significantly between POM size fractions (ANOVA; $p < 0.001$). A post hoc Tukey HSD test found significant differences for all pairwise comparisons ($p < 0.05$). Similar to δ^{15}N, POM δ^{13}C values were lowest for the picosize fraction (ave. $= -24.70$‰) (Figure 6). However, average values were consistently higher in the nanosize fraction (ave. $= -21.97$‰) compared to the microsize fraction (ave. $= -23.17$‰). Zooplankton δ^{13}C values averaged -21.27‰ in winter, -21.75‰ in SpringHB, and -22.68‰ in SpringLB. A weak increasing trend in δ^{13}C values was observed across zooplankton size classes.

3.4. Mixing Model Outputs
Biplots illustrating the distribution of POM size fraction values relative to zooplankton consumer groups are provided in supporting information Figure S2. The mixing model estimated that in winter the pico-POM contributed 28.4%, the nano-POM 58.3%, and the micro-POM 14.9% on average to zooplankton biomass (Figure 7). These contributions were consistent across size classes.
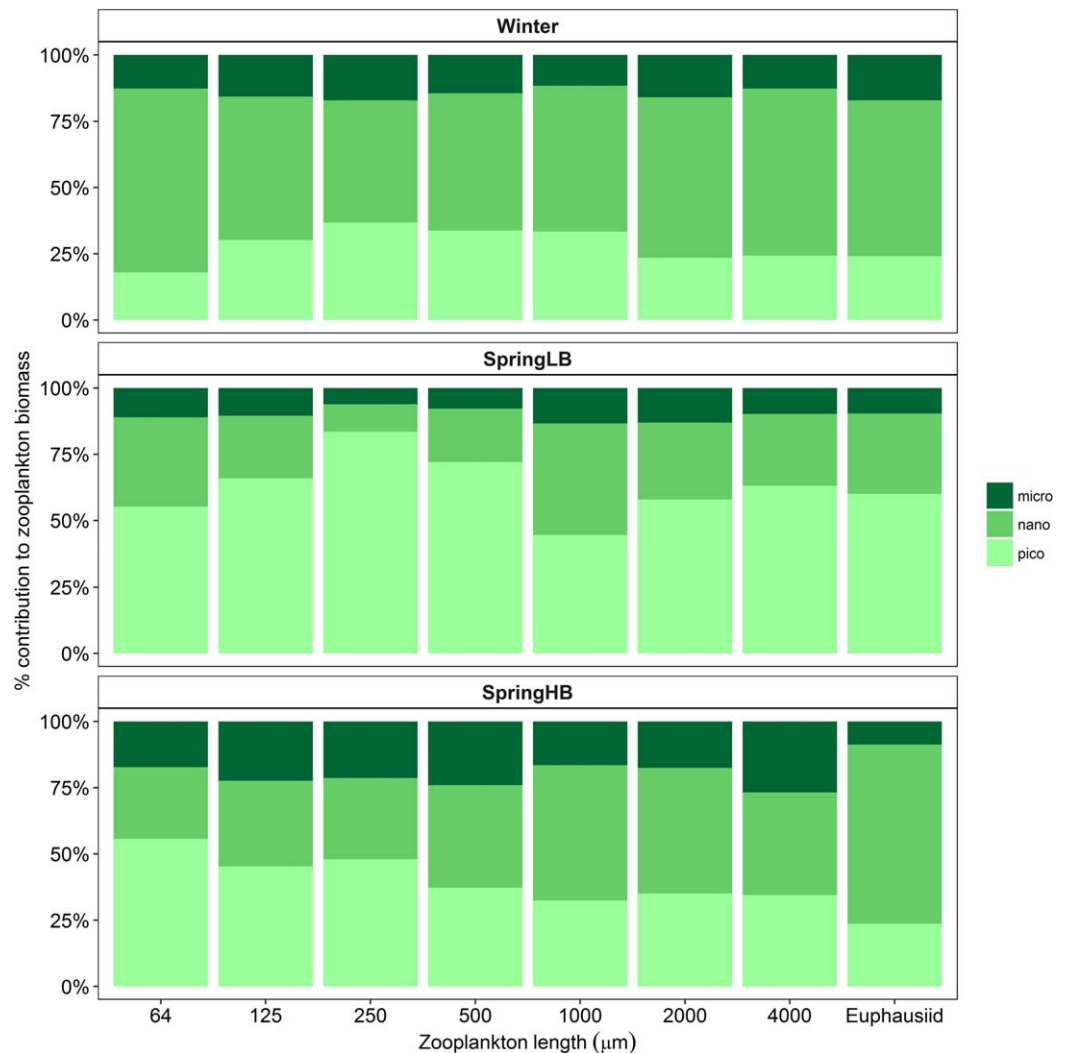
Figure 7. Estimates of percent contribution of pico-POM, nano-POM, and micro-POM to zooplankton biomass based on the simmr Bayesian mixing model output for winter, SpringLB, and SpringHB. The model applied trophic discrimination factor values from a global meta-analysis of 2.75 ($\pm$0.1) for δ^{15}N and 0.75 ($\pm$0.11) for δ^{13}C [*Caut et al.*, 2009].

Correlations between contributions for pairs of potential food sources (POM size fractions) are presented in supporting information Figure S2. Large negative correlations indicate that food sources are difficult to distinguish. In the winter, the highest negative correlations (>-0.8) were observed between pico-POM and nano-POM with respect to the 2000 and 4000 μm zooplankton size classes (supporting information Figure S2.1).

In the spring, the contributions of pico-POM, nano-POM, and micro-POM differed markedly between SpringLB and SpringHB (Figure 7). In SpringHB, pico-POM contributed 40.3%, the nano-POM 43.1%, and the micro-POM 20.1% on average to zooplankton biomass. The contribution of pico-POM was highest in the 64 μm zooplankton size class (57%) and decreased with increasing size class. Conversely, the nano-POM contribution increased with increasing zooplankton size class, with a maximum for euphausiids of 68.9%. High negative correlations (>-0.8) were observed between pico-POM and nano-POM size fractions for the 2000 μm zooplankton size class and euphausiids (supporting information Figure S2.2).

In SpringLB, pico-POM contributed 64.1%, nano-POM 27.7%, and micro-POM 10.4% on average to zooplankton biomass. The contribution of nanoplankton was highest in the >1000 μm size class (ave. = 33%). Negative correlations of >-0.9 were observed between pico-POM and nano-POM size classes for model runs for all eight zooplankton groups, indicating that the relative contributions of these two groups were not well resolved.

4. Discussion

4.1. The Plankton Food-Web Structure

The 2013 DEWEX program coincided with a winter of exceptionally deep convection in the Liguro-Provencal Basin, the physics of which are described in detail elsewhere [*Houpert et al.*, 2016]. Phytoplankton biomass was uniformly low during the winter survey with equal contributions of picophytoplankton, nanophytoplankton, and microphytoplankton biomass. By the time of the spring survey, a bloom was in progress in the deep convection zone, attributed to high productivity of both nanophytoplankton and the diatom dominated microphytoplankton size class [*Mayot et al.*, 2017]. Conversely, outside the convection zone, spring phytoplankton biomass was weakly elevated and dominated by nanophytoplankton. The spring phytoplankton community composition could therefore be divided between stations with characteristics of eutrophic temperate systems (high biomass/high microphytoplankton), and stations more typical of oligotrophic systems (low biomass/low microphytoplankton) [*Kiorboe*, 1993]. The winter to spring transition period therefore provided an excellent case study for testing the relative contributions of picophytoplankton, nanophytoplankton, and microplankton to zooplankton biomass under contrasting trophic regimes.

The zooplankton community taxonomic composition is discussed in detail in *Donoso et al.* [2017]. That study found that copepods contributed ∼95% to total zooplankton abundance. Our size fractionated analysis confirmed the high dominance of copepods in the 64–1000 μm size fractions, while in the $\geq$2000 μm fractions euphausiids, gelatinous predators, and tunicates were important contributors. The smallest zooplankton size classes (64–250 μm) were the largest contributors to total abundance. A substantial increase in the densities of the 250 μm size class between winter and spring, also apparent in the biomass data, reflected enhanced spring secondary production. A similar increase was also observed in the biomass of the calanoid dominated 500 and 1000 μm size classes. Total zooplankton biomass levels were significantly higher in the SpringHB and SpringLB zones than in winter but were highest in the SpringHB. In summary, the stations sampled during the two DEWEX surveys could be divided into three distinct trophic groupings: (1) a winter food web with low phytoplankton biomass, with equal contributions of picophytoplankton, nanophytoplankton, and microphytoplankton, and low zooplankton biomass; (2) a low biomass spring food web located in the region outside the convection zone, not subject to deep nutrient renewal, with elevated nanophytoplankton but low microphytoplankton biomass and zooplankton biomass elevated relative to winter levels; and (3) the high nutrient high productivity convection zone, with high nanophytoplankton, microphytoplankton, and zooplankton biomass.

4.2. Stable Isotope Values of POM

A remarkable feature of the POM stable isotope data in this study was the substantial difference between size classes, increasing from the picofractions to microfractions. We measured a 4–6‰ difference in δ^{15}N between the pico-POM and micro-POM size fractions, which compares well with data from the Southern Ocean (4–6‰) [*Karsh et al.*, 2003], Sea of Japan (4–5‰) [*Im and Suh*, 2016], North Sea (1–2‰) [*Tiselius and Fransson*, 2016], and Mediterranean (1–6‰) [*Rau et al.*, 1990]. δ^{13}C also differed substantially between POM fractions (1.5–4.5‰), though unlike δ^{15}N the highest values were always measured for the nanosize fraction. Similarly, the differences observed in this study were within the range of data from the Sea of Japan (1.5–6‰) [*Im and Suh*, 2016], North Sea (1.5–2‰) [*Tiselius and Fransson*, 2016], and Mediterranean (3–6‰) [*Rau et al.*, 1990]. POM is a mixture of autotrophic and heterotrophic material and one possible explanation for the increased POM δ values with increasing size is therefore heterotrophic enrichment of ^{15}N and ^{13}C. If this were the case one would expect a similar increase in δ values for both carbon and nitrogen, yet this was not the case in this study. Observations of minimal isotopic fractionation between phytoplankton and microzooplankton provides further evidence that fractionation was not the driver of differences in POM size fraction isotope values [*Gutiérrez-Rodríguez et al.*, 2014]. *Karsh et al.* [2003] measured an increase in δ^{15}N with POM size fractions despite all size fractions being dominated by autotrophs, suggesting that autotrophic processes were the cause of variations in POM δ. These authors suggested that differences in the forms of nitrogen assimilated by phytoplankton groups may be an important contributing factor. Indeed, preferential uptake of ammonium and urea has been measured for picophytoplankton and nanophytoplankton size classes, accounting for 75% and 62% of their production, respectively [*Probyn and Painting*, 1985]. Ammonium has a lower δ^{15}N than nitrate and a higher fractionation factor [*Pennock et al.*, 1996].

Preferential uptake of ammonium is therefore the most likely explanation for the depleted ^{15}N in smaller phytoplankton size classes in our study.

4.3. Plankton Food-Web Linkages

The consistent difference in stable isotope ratios between pico-POM, nano-POM, and micro-POM size classes made them excellent candidates for mixing model analysis of their relative contributions to zooplankton biomass [*Phillips et al.*, 2014]. Overall, model estimates of relative contributions largely reflected the variations in biomass of picophytoplankton, nanophytoplankton, and microphytoplankton biomass between the winter, SpringLB, and SpringHB zones. In the winter, nano-POM made the largest contribution to zooplankton biomass. In the spring, the high productivity SpringHB zone was characterized by the largest percent contribution of micro-POM to zooplankton biomass, while in the low productivity SpringLB region pico-POM was identified as the dominant contributor to the biomass of all zooplankton size classes. We combined zooplankton group composition (Figure 4) with the mixing model output (Figure 7) to summarize plankton food-web linkages for the three food-web scenarios in the Liguro-Provencal Basin outlined above (Figure 8). In the winter, micro-POM contributed an average of 15% to total zooplankton biomass. The contribution of pico-POM and nano-POM was consistent for all zooplankton size classes and averaged 28% for the former and 59% for the latter. Phytoplankton biomass in the SpringLB area did not differ significantly from winter levels and here pico-POM was estimated to have made an even larger contribution to total zooplankton biomass (62–68%). Nano-POM contributed an average of 28% and micro-POM 10% to zooplankton biomass. We caution that the model did not differentiate well between pico-POM and nano-POM in the SpringLB, leaving some uncertainty as to the relative contributions of these two size fractions. Compared to the SpringLB zone, there was a more even contribution to total zooplankton biomass by pico-POM (ave. = 42%), nano-POM (ave. = 42%), and micro-POM (ave. = 20%) in the SpringHB area. The proportional contributions of POM
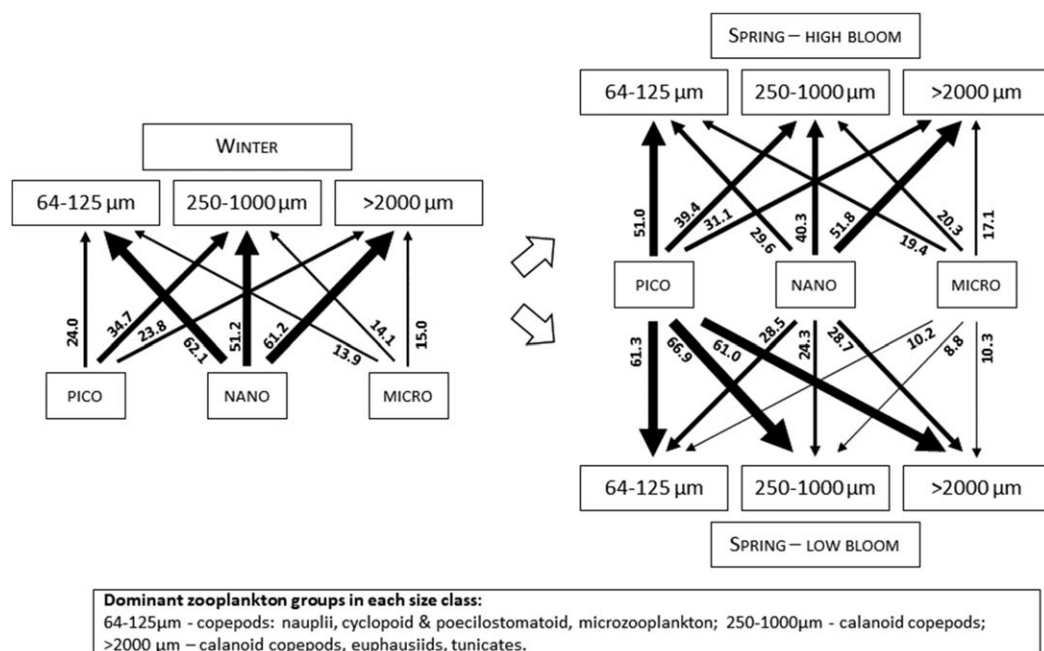

Dominant zooplankton groups in each size class:
64-125µm - copepods: nauplii, cyclopoid & poecilostomatoid, microzooplankton; 250-1000µm - calanoid copepods; >2000 µm – calanoid copepods, euphausiids, tunicates.

Figure 8. Relative contributions picoplankton, nanoplankton, and microplankton biomass to the biomass of three zooplankton size fractions in the Liguro-Provencal Basin in WINTER and SpringHB and SpringLB based on isotope mixing model outputs (see section 2 and Figure 7). Arrows indicate the transfer of material between pico-POM, nano-POM, and micro-POM fractions and zooplankton size classes, and their thickness is proportional to relative contribution. Values of percentage contributions determined from the mixing model are located against the corresponding arrow. Winter was a period of low phytoplankton biomass across all size fractions; SpringHB is representative of the deep convection zone in the central basin with high nutrients and high phytoplankton biomass dominated by nanophytoplankton and microphytoplankton; and SpringLB is representative of the region outside the convection zone dominated by nanophytoplankton. Zooplankton size classes: 64–125 μm—copepods: nauplii, cyclopoid, and poecilostomatoid; 250–1000 μm—calanoid: copepods; >2000 μm—calanoid: copepods, euphausiids, tunicates, gelatinous predators, and amphipods.

size fractions to zooplankton biomass decreased with increasing zooplankton size for pico-POM, increased with increasing zooplankton size for nano-POM, and remained relatively constant across zooplankton size groups for micro-POM.

The estimated average pico-POM contributions to zooplankton in the low phytoplankton biomass winter and SpringLB zones were 28 and 64%, respectively. Although the nano-POM contribution may have been underestimated in the SpringLB, the pico-POM contribution in this zone was similar to the previously estimated 50% picophytoplankton contribution in oligotrophic systems [*Calbet and Saiz*, 2005]. Since picoplankton are too small to be effectively grazed by most metazoans [*Fortier et al.*, 1994], it is expected that the dominant pathway of picoplankton to the zooplankton is via the intermediary steps of nanoflagellates and ciliates [*Christaki et al.*, 2001; *Sommer et al.*, 2002]. Notably, nanoflagellate density was an order of magnitude higher in the SpringLB than the winter zone, and this functional group may have facilitated the higher transfer of picoplankton biomass to the zooplankton in the former. Similarly, high nanoflagellate biomass in the SpringHB area may have contributed to the relatively large contribution of pico-POM to zooplankton biomass in this zone, despite the high nanoplankton and microplankton biomass. Our estimated 42% pico-POM contribution in the SpringHB exceeded the previously suggested 25% for eutrophic systems [*Calbet and Saiz*, 2005]. It is likely that omnivorous feeding by the larger zooplankton size fractions on smaller zooplankton fractions and microzooplankton contributed to the transfer of picoplankton biomass. Although the contribution of micro-POM to zooplankton biomass was highest in the SpringHB, its maximum contribution was 29% in the 4000 μm zooplankton fraction, despite microphytoplankton making up 44% of the phytoplankton biomass in this zone. This finding indicated that a large part of the microphytoplankton biomass may have remained ungrazed during our study. This suggestion is supported by studies that have demonstrated selection against diatoms (which dominate the microphytoplankton size fraction) by zooplankton grazers [*Atkinson*, 1996; *Kleppel et al.*, 1991], in response to diatom structural defenses [*Raven and Waite*, 2004], chemical defenses [*Miralto et al.*, 1999], and high silicate content [*Liu et al.*, 2016]. The Si:N ratios of diatoms can increase both in response to grazing [*Pondaven et al.*, 2007] and during bloom periods [*Saito and Tsuda*, 2003] and were therefore expected to have been higher in the SpringHB.

5. Conclusions

Stable isotopes provide a powerful tool for the analysis of the contribution of organic matter sources to food webs [*Layman et al.*, 2012]. Here we have combined size structured stable isotope analysis of the plankton food web in the north-west Mediterranean with a Bayesian mixing model framework to estimate the relative contributions of picosize, nanosize, and microsize POM to zooplankton biomass during winter, and in contrasting high and low productivity spring conditions. Our findings support an important role for picoplankton in oligotrophic ecosystems. We estimated an average 64% contribution by this size class to zooplankton biomass in the spring low productivity region of the north-west Mediterranean in our study. Although the model did not differentiate well between pico-POM and nano-POM in the spring low productivity region, these reported values are in the range of previous estimates [*Calbet and Saiz*, 2005]. Significantly, the estimated contribution of picoplankton to zooplankton biomass in the high productivity spring region remained high, averaging 42% across zooplankton size classes. This has implications for concepts of zooplankton food-web structure, suggesting that the role of diatoms may at times be overestimated, and a greater importance for the microbial loop in eutrophic environments [*Legendre and Rassoulzadegen*, 1995]. Furthermore, high transfer of picoplankton to zooplankton has implications for the cycling of biomass within the photic zone and vertical flux pathways, with picoplankton potentially making a higher contribution to the latter than expected [*Kiorboe*, 1993], via zooplankton fecal pellet production. What our stable isotope approach does not reveal is the detailed pathways of food-web sources to the zooplankton. Nanoheterotrophs likely play a significant role in linking the picoplankton to the zooplankton, pointing to the importance of complex lower trophic level interactions in mediating organic matter transfer [*Legendre and Rassoulzadegen*, 1995]. Resolving these pathways represents an important research avenue with respect to understanding the functioning of plankton food webs and their response to changing ocean conditions. Developments in compound specific isotope analysis [*Bec et al.*, 2011; *Larsen et al.*, 2013] and DNA-based dietary studies [*Durbin and Casas*, 2014] offer new approaches that may enable significant advancements in this field.

References

Atkinson, A. (1996), Subantarctic copepods in an oceanic, low chlorophyll environment: Ciliate predation, food selectivity and impact on prey populations, *Mar. Ecol. Prog. Ser.*, *130*, 85–96, doi:10.3354/meps130085.

Azam, F., T. Fenchel, J. G. Field, J. S. Gray, L. A. Meyer-Reil, and F. Thingstad (1983), The ecological role of water-column microbes in the sea, *Mar. Ecol. Prog. Ser.*, *10*, 257–263.

Barnes, C., D. Maxwell, D. C. Reuman, and S. Jennings (2010), Global patterns in predator-prey size relationships reveal size dependency of trophic transfer efficiency, *Ecology*, *91*(1), 222–232.

Bec, A., M.-E. Perga, A. Koussoroplis, G. Bardoux, C. Desvilettes, G. Bourdier, and A. Mariotti (2011), Assessing the reliability of fatty acid-specific stable isotope analysis for trophic studies, *Methods Ecol. Evol.*, *2*(6), 651.

Boyce, D. G., K. T. Frank, and W. C. Leggett (2015), From mice to elephants: Overturning the 'one size fits all' paradigm in marine plankton food chains, *Ecol. Lett.*, *18*(6), 504–515, doi:10.1111/ele.12434.

Calbet, A., and M. R. Landry (1999), Mesozooplankton influences on the microbial food web: Direct and indirect trophic interactions in the oligotrophic open ocean, *Limnol. Oceanogr.*, *44*(6), 1370–1380.

Calbet, A., and M. R. Landry (2004), Phytoplankton growth, microzooplankton grazing, and carbon cycling in marine systems, *Limnol. Oceanogr.*, *49*(1), 51.

Calbet, A., and E. Saiz (2005), The ciliate-copepod link in marine ecosystems, *Aquat. Microb. Ecol.*, *38*(2), 157–167, doi:10.3354/ame038157.

Caut, S., E. Angulo, and F. Courchamp (2009), Variation in discrimination factors (δ^{15}N and δ^{13}C): The effect of diet isotopic values and applications for diet reconstruction, *J. Appl. Ecol.*, *46*(2), 443–453, doi:10.1111/j.1365-2664.2009.01620.x.

Christaki, U., A. Giannakourou, F. Van Wambeke, and G. Grégori (2001), Nanoflagellate predation on auto- and heterotrophic picoplankton in the oligotrophic Mediterranean Sea, *J. Plankton Res.*, *23*(11), 1297–1310, doi:10.1093/plankt/23.11.1297.

Clarke, K. R., and R. M. Warwick (2001), A further biodiversity index applicable to species lists: Variation in taxonomic distinctness, *Mar. Ecol. Prog. Ser.*, *216*, 265–278.

Cohen, J. E., S. L. Pimm, P. Yodzis, and J. Salda (1993), Body sizes of animal predators and animal prey in food webs, *J. Anim. Ecol.*, *62*(1), 67–78.

Craig, C., W. J. Kimmerer, and C. S. Cohen (2014), A DNA-based method for investigating feeding by copepod nauplii, *J. Plankton Res.*, *36*(1), 271–275, doi:10.1093/plankt/fbt104.

Donoso, K., F. Carlotti, M. Pagano, B. P. V. Hunt, R. Escribano, and L. Berline (2017), Zooplankton community response to the winter 2013 deep convection process in the NW Mediterranean Sea, *J. Geophys. Res. Oceans*, *122*), 2319–2338, doi:10.1002/2016JC012176.

D'Ortenzio, F., and M. Ribera d'Alcalà (2009), On the trophic regimes of the Mediterranean Sea: A satellite analysis, *Biogeosciences*, *6*(2), 139–148, doi:10.5194/bg-6-139-2009.

Durbin, E. G., and M. C. Casas (2014), Early reproduction by *Calanus glacialis* in the Northern Bering Sea: The role of ice algae as revealed by molecular analysis, *J. Plankton Res.*, *36*(2), 523–541, doi:10.1093/plankt/fbt121.

El-Sabaawi, R., J. Dower, M. Kainz, and A. Mazumder (2009), Characterizing dietary variability and trophic positions of coastal calanoid copepods: Insight from stable isotopes and fatty acids, *Mar. Biol.*, *156*(3), 225.

Escribano, R., and C. S. Pérez (2010), Variability in fatty acids of two marine copepods upon changing food supply in the coastal upwelling zone off Chile: Importance of the picoplankton and nanoplankton fractions, *J. Mar. Biol. Assoc. U. K.*, *90*(2), 301–313, doi:10.1017/S002531540999083X.

Estrada, M., M. Latasa, M. Emelianov, A. Gutiérrez-Rodríguez, B. Fernández-Castro, J. Isern-Fontanet, B. Mouriño-Carballido, J. Salat, and M. Vidal (2014), Seasonal and mesoscale variability of primary production in the deep winter-mixing region of the NW Mediterranean, *Deep Sea Res., Part I*, *94*, 45–61, doi:10.1016/j.dsr.2014.08.003.

Field, J. G., K. R. Clarke, and R. M. Warwick (1982), A practical strategy for analysing multispecies distribution patterns, *Mar. Ecol. Prog. Ser.*, *8*, 37–52.

Fileman, E. S., P. K. Lindeque, R. A. Harmer, C. Halsband, and A. Atkinson (2014), Feeding rates and prey selectivity of planktonic decapod larvae in the Western English Channel, *Mar. Biol.*, *161*(11), 2479–2494, doi:10.1007/s00227-014-2520-9.

Finkel, Z. V., J. Beardall, K. J. Flynn, A. Quigg, T. A. V. Rees, and J. A. Raven (2010), Phytoplankton in a changing world: Cell size and elemental stoichiometry, *J. Plankton Res.*, *32*(1), 119–137, doi:10.1093/plankt/fbp098.

Fortier, L., J. Le Fevre, and L. Legendre (1994), Export of biogenic carbon to fish and to the deep ocean: The role of large planktonic microphages, *J. Plankton Res.*, *16*(7), 809–839, doi:10.1093/plankt/16.7.809.

Ganachaud, A., A. Sen Gupta, J. Brown, K. Evans, C. Maes, L. Muir, and F. Graham (2013), Projected changes in the tropical Pacific Ocean of importance to tuna fisheries, *Clim. Change*, *119*(1), 163–179.

Gifford, D. J., and D. A. Caron (2000), Sampling, preservation, enumeration and biomass of marine protozooplankton, in *ICES Zooplankton Methodology Manual*, edited by P. Wiebe et al., pp. 193–221, Academic, London.

Gutiérrez-Rodríguez, A., M. Décima, B. N. Popp, and M. R. Landry (2014), Isotopic invisibility of protozoan trophic steps in marine food webs, *Limnol. Oceanogr.*, *59*(5), 1590–1598, doi:10.4319/lo.2014.59.5.1590.

Hobson, K. A., and H. E. Welch (1992), Determination of trophic relationships within a high Arctic marine food web using δ^{13}C and δ^{15}N analysis, *Mar. Ecol. Prog. Ser.*, *84*, 9–18.

Houpert, L., X. Durrieu de Madron, P. Testor, A. Bosse, F. D'Ortenzio, M. Bouin, D. Dausse, H. Le Goff, S. Kunesch, and M. Labaste (2016), Observations of open-ocean deep convection in the northwestern Mediterranean Sea: Seasonal and interannual variability of mixing and deep water masses for the 2007–2013 Period, *J. Geophys. Res. Oceans*, *121*, 8139–8171, doi:10.1002/2016JC011857.

Im, D.-H., and H.-L. Suh (2016), Ontogenetic feeding migration of the euphausiid *Euphausia pacifica* in the East Sea (Japan Sea) in autumn: A stable isotope approach, *J. Plankton Res.*, *38*(4), 904–914, doi:10.1093/plankt/fbw041.

Karsh, K. L., T. Trull, M. Lourey, and D. Sigman (2003), Relationship of nitrogen isotope fractionation to phytoplankton size and iron availability during the Southern Ocean Iron RElease Experiment (SOIREE), *Limnol. Oceanogr.*, *48*(3), 1058–1068.

Kiorboe, T. (1993), Turbulence, phytoplankton cell size, and the structure of pelagic food webs, *Adv. Mar. Biol.*, *29*, 1–72.

Kleppel, G. S., D. Holliday, and R. Pieper (1991), Trophic interactions between copepods and microplankton: A question about the role of diatoms, *Limnol. Oceanogr.*, *36*(1), 172–178.

Larsen, T., M. Ventura, N. Andersen, D. M. O'Brien, U. Piatkowski, and M. D. McCarthy (2013), Tracing carbon sources through aquatic and terrestrial food webs using amino acid stable isotope fingerprinting, *PLoS ONE*, *8*(9), e73441, doi:10.1371/journal.pone.0073441.

Layman, C. A., et al. (2012), Applying stable isotopes to examine food-web structure: An overview of analytical tools, *Biol. Rev.*, *87*(3), 545.

Legendre, L., and F. Rassoulzadegan (1995), Plankton and nutrient dynamics in marine waters, *Ophelia*, *41*, 153–172.

Lewandowska, A., and U. Sommer (2010), Climate change and the spring bloom: A mesocosm study on the influence of light and temperature on phytoplankton and mesozooplankton, *Mar. Ecol. Prog. Ser.*, *405*, 101–111, doi:10.3354/meps08520.

Liu, H., M. Chen, F. Zhu, and P. J. Harrison (2016), Effect of diatom silica content on copepod grazing, growth and reproduction, *Frontiers Mar. Sci.*, *3*, 89, doi:10.3389/fmars.2016.00089.

Marty, J.-C., J. Chiavérini, M.-D. Pizay, and B. Avril (2002), Seasonal and interannual dynamics of nutrients and phytoplankton pigments in the western Mediterranean Sea at the DYFAMED time-series station (1991–1999), *Deep Sea Res., Part II*, *49*(11), 1965.

Mayot, N., F. D'Ortenzio, J. Uitz, B. Gentili, J. Ras, V. Vellucci, M. Golbol, D. Antoine, and H. Claustre (2017), Influence of the phytoplankton community structure on the spring and annual primary production in the North-Western Mediterranean Sea, *J. Geophys. Res. Oceans*, doi:10.1002/2016JC012668, in press.

Miralto, A., G. Barone, G. Romano, S. Poulet, A. Ianora, G. Russo, I. Buttino, G. Mazzarella, M. Laabir, and M. Cabrini (1999), The insidious effect of diatoms on copepod reproduction, *Nature*, *402*(6758), 173–176.

Moran, X. A. G., A. Lopez-Urrutia, A. Calvo-Diaz, and W. K. W. Li (2010), Increasing importance of small phytoplankton in a warmer ocean, *Global Change Biol.*, *16*(3), 1137–1144.

Parnell, A. C., D. L. Phillips, S. Bearhop, B. X. Semmens, E. J. Ward, J. W. Moore, A. L. Jackson, J. Grey, D. J. Kelly, and R. Inger (2013), Bayesian stable isotope mixing models, *Environmetrics*, *24*(6), 387–399, doi:10.1002/env.2221.

Pennock, J. R., D. J. Velinsky, J. M. Ludlam, J. H. Sharp, and M. L. Fogel (1996), Isotopic fractionation of ammonium and nitrate during uptake by *Skeletonema costatum*: Implications for δ15N dynamics under bloom conditions, *Limnol. Oceanogr.*, *41*(3), 451–459, doi:10.4319/lo.1996.41.3.0451.

Phillips, D. L., R. Inger, S. Bearhop, A. L. Jackson, J. W. Moore, A. C. Parnell, B. X. Semmens, and E. J. Ward (2014), Best practices for use of stable isotope mixing models in food-web studies, *Can. J. Zool.*, *92*(10), 823–835, doi:10.1139/cjz-2014-0127.

Polovina, J. J., J. P. Dunne, P. A. Woodworth, and E. A. Howell (2011), Projected expansion of the subtropical biome and contraction of the temperate and equatorial upwelling biomes in the North Pacific under global warming, *ICES J. Mar. Sci.*, *68*(6), 986–995, doi:10.1093/icesjms/fsq198.

Pondaven, P., M. Gallinari, S. Chollet, E. Bucciarelli, G. Sarthou, S. Schultes, and F. Jean (2007), Grazing-induced changes in cell wall silicification in a marine diatom, *Protist*, *158*(1), 21–28.

Probyn, T. A., and S. J. Painting (1985), Nitrogen uptake by size-fractionated phytoplankton populations in Antarctic surface waters, *Limnol. Oceanogr.*, *30*(6), 1327–1332, doi:10.4319/lo.1985.30.6.1327.

R Core Team (2016), *R: A Language and Environment for Statistical Computing*, R Found. for Stat. Comput., Vienna.

Rau, G. H., J. L. Teyssie, F. Rassoulzadegan, and S. W. Fowler (1990), ^{13}C/^{12}C and ^{15}N/^{14}N variations among size fractionated marine particles: Implications for their origin and trophic relationships, *Mar. Ecol. Prog. Ser.*, *59*, 33–38.

Rautio, M., and W. F. Vincent (2007), Isotopic analysis of the sources of organic carbon for zooplankton in shallow subarctic and arctic waters, *Ecography*, *30*(1), 77–87.

Raven, J., and A. Waite (2004), The evolution of silicification in diatoms: Inescapable sinking and sinking as escape?, *New Phytol.*, *162*(1), 45–61.

Rossi, S., A. Sabatés, M. Latasa, and E. Reyes (2006), Lipid biomarkers and trophic linkages between phytoplankton, zooplankton and anchovy (*Engraulis encrasicolus*) larvae in the NW Mediterranean, *J. Plankton Res.*, *28*(6), 551–562, doi:10.1093/plankt/fbi140.

Ryther, J. H. (1969), Photosynthesis and fish production in the sea, *Science*, *166*(3901), 72–76.

Saito, H., and A. Tsuda (2003), Influence of light intensity on diatom physiology and nutrient dynamics in the Oyashio region, *Prog. Oceanogr.*, *57*(3–4), 251–263, doi:10.1016/S0079-6611(03)00100-9.

Schukat, A., H. Auel, L. Teuber, N. Lahajnar, and W. Hagen (2014), Complex trophic interactions of calanoid copepods in the Benguela upwelling system, *J. Sea Res.*, *85*, 186–196, doi:10.1016/j.seares.2013.04.018.

Sheldon, R. W., A. Prakash, and W. H. Sutcliffe Jr. (1972), The size distribution of particles in the ocean, *Limnol. Oceanogr.*, *17*(3), 327.

Siokou-Frangou, I., U. Christaki, M. G. Mazzocchi, M. Montresor, M. Ribera d'Alcalá, D. Vaqué, and A. Zingone (2010), Plankton in the open Mediterranean Sea: A review, *Biogeosciences*, *7*(5), 1543–1586, doi:10.5194/bg-7-1543-2010.

Sommer, U., H. Stibor, A. Katechakis, F. Sommer, and T. Hansen (2002), Pelagic food web configurations at different levels of nutrient richness and their implications for the ratio fish production: Primary production, *Hydrobiologia*, *484*(1), 11–20.

Tiselius, P., and K. Fransson (2016), Daily changes in δ15N and δ13C stable isotopes in copepods: Equilibrium dynamics and variations of trophic level in the field, *J. Plankton Res.*, *38*(3), 751–761, doi:10.1093/plankt/fbv048.

Uitz, J., H. Claustre, A. Morel, and S. B. Hooker (2006), Vertical distribution of phytoplankton communities in open ocean: An assessment based on surface chlorophyll, *J. Geophys. Res.*, *111*, C08005, doi:10.1029/2005JC003207.

Uitz, J., H. Claustre, B. Gentili, and D. Stramski (2010), Phytoplankton class-specific primary production in the world's oceans: Seasonal and interannual variability from satellite observations, *Global Biogeochem. Cycles*, *24*(3), GB3016, doi:10.1029/2009GB003680.

Wada, E., H. Mizutani, and M. Minagawa (1991), The use of stable isotopes for food web analysis, *Crit. Rev. Food Sci. Nutr.*, *30*, 361–371.

Waite, A. M., B. A. Muhling, C. M. Holl, L. E. Beckley, J. P. Montoya, J. Strzelecki, P. A. Thompson, and S. Pesant (2007), Food web structure in two counter-rotating eddies based on δ^{15}N and δ^{13}C isotopic analyses, *Deep Sea Res., Part II*, *54*, 1055–1075.

Erratum

In the originally published version of this article, Figure 8 displayed five incorrect percentage values. The figure has since been corrected, and this version may be considered the authoritative version of record.